A Study of the Effect of Symmetric and Asymmetric Design for CRLH-TL Unit Cell on XPD and Isolation for Dual Linear Polarized Antenna at Different Values of Phase Shifts

Sadiq Ahmed[*1,2], and Madhukar Chandra[1]

[1]Microwave Engineering and Electromagnetic Theory, TU Chemnitz, Chemnitz, Germany
[2]Electrical Engineering Department, Engineering College, University of Mustansiriyah, Baghdad, Iraq
[*]email: sadiq-kadhim-ahmed.aqbi@s2013.tu-chemnitz.de

***Abstract* — Dual linear polarization antennas with low cross polarization have been widely used for synthetic aperture radar and wireless communication applications. This work presents a new design of a dual linear polarization single microstrip patch antenna with low cross-polarization pattern and high isolation between two input ports. The work has two main objectives. The first is to generate different values of phase shifts (0^o-90^o) using composite right left transmission line (CRLH-TL) metamaterial (symmetric and asymmetric configurations), in order to investigate the cross-polarization discrimination (XPD) and isolation between the two input ports for a dual linear polarized antenna at the frequency of 10 GHz. The simulation reveals that the XPD of 34 dB and isolation of -30 dB at a phase shift of 40^o. This method results in significant improvement in co-cross polarization discrimination at the phase shift of 40^o in comparison to the conventional antenna. The simulation, in this regard, reveals an improvement of 7 dB in principle planes (E and H). The second objective is a comparative study between the symmetric and asymmetric unit cells and their effects on the cross polarization patterns. Furthermore, we report on the effect of phase shift on the other characteristics such as gain and bandwidth. The simulations are evaluated utilizing the commercial full-wave simulator Ansoft High-Frequency Structure Simulator (HFSS).**

Keywords - dual linear polarization; composite right- left-hand transmission line metamaterials

I. INTRODUCTION

Dual linear polarization microstrip antenna is common and ideally suited for good performance wireless communication, satellite, and radar applications, particularly for synthetic aperture radar (SAR) application. This is because dual linear polarization antennas offer to increase the capacity and thus enhance the accuracy of identifying objects [1]. On the other hands, a dual linear polarization antenna suffers from the two drawbacks. The first is related to the mutual coupling between two input ports and the second is related to the cross polarization pattern. Therefore, studying and obtaining of these characteristics for the dual linear polarization antennas are an important work in antenna design, especially for weather radar and mobile communication applications. Therefore, how to reduce the cross-polarization pattern and to obtain high isolation for the dual linear polarization becomes an important topic and they are considered the key points for operation of dual linear polarization antenna system [2]. Many efforts have been made to implement of a dual linear polarization patch antenna for reduction of mutual coupling between two input ports and cross polarization discrimination enhancement in the past few decades[3][4].

Dual linear polarization antenna can be achieved by using patch antenna with two orthogonal feeds which placed in horizontal and vertical positions to produce dual linear polarization operation. There are several feeding mechanisms available for a dual linear polarization antenna. The related feeding techniques are aperture coupling with different shapes of slots (such as straight narrow slots, two offset narrow slots, cross-shaped slots, and bone slots), proximity coupling, insert feeding, probe feeding, and capacitively coupled feed [2][3][4][5].

Theoretically, the dual linear polarizations are normally referred to as vertical and horizontal ports and they are completely isolated between them. This leads to polarization purity. On the other hand, in practically the polarization directions are tilted somewhat from local vertical and horizontal references, this leads to polarization impurity (generate cross polarization patterns and this phenomenon, it is unavoidable). Fig.(1) shows the shifting in polarization references. To solve this problem, phase shift technique is used to compensate shifting in the phase. Utilizing of unique properties of CRLH-TL metamaterial phase shifter to produce the positive phase shift and thus reducing the cross polarization patterns. In this work, metamaterial line feed is used as a new feed technique and it works as a horizontal port. Moreover, it also works as a phase shifter.

This paper proposes a simple design of dual-linear polarization single microstrip patch antenna fed by two-hybrid feeds. Also, it has two configurations of unit cells; symmetric and asymmetric. The CRLH-TL metamaterial unit cell generates different values of phase shifts (0^o-90^o), in order to investigate the cross-polarization discrimination and isolation between the two input ports for a dual linear polarization antenna at the centre frequency of 10 GHz.

Furthermore, there is a comparison between symmetric and asymmetric design for CRLH-TL unit cell and discuss their effects on the XPD and isolation between the two input ports. Additionally, it has been studied the effect of the phase shift on another characteristic such as gain and bandwidth. This paper is organized as follows: Section 2 deals with cross polarization sources, section 3 is the design of CRLH-TL symmetric and an asymmetric metamaterial, section 4 is phase shifter design using CRLH-TL metamaterial, section 5 is implementation of a dual linear polarization rectangular microstrip antenna, section 6 is related to the results and discussion, section 7 deals with the study the effects of phase shifts on isolation and cross polarization pattern, and section 8 contains conclusions.

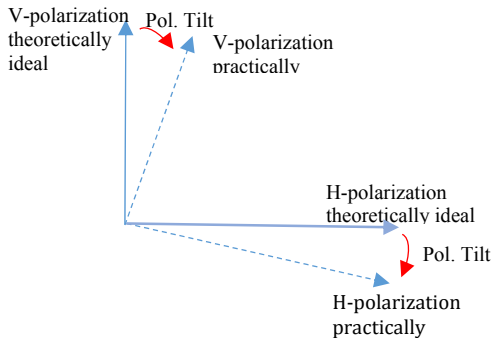

Figure 1. V and H polarization in view of theoretically and practically.

II. Cross- Polarization Sources for a Dual Linear Polarization Antennas

The cross polarization discrimination (XPD) is defined as a measure of the degree of interference (cross-coupling) between dual linear polarized channels. Alternatively, in other words, the XPD, which is the ratio of the electric field received with the co-polarization to the electric field received with the orthogonal polarization at the reception [6]. It can be expressed in dB as follow:

$$XPD = 20 \log \frac{E_{vv}}{E_{vh}} \quad (1)$$

where E_{ij} is the amplitude of the electric field at the receiver that is transmitted in polarization state i and received in the perpendicular polarization state j (i,j=l,2). The co-polarized refers to identical transmit and receive polarization (E_{vv} and E_{hh}). The cross polarization refers to transmitting in one polarization state i, and receiving in the orthogonal polarization state j, (E_{vh} and E_{hv}), where v and h refer to vertical and horizontal ports, respectively [7].

There are many sources that generate cross polarization patterns and mutual coupling between two input ports in dual linear polarization. The higher modes become one of the main sources of the cross polarization pattern and mutual coupling in dual linear polarized antennas[8], the second important factor for generating cross-polarization radiation is related to the symmetry of antenna system with respect to the two principal planes which consists of the geometry of the patch antenna and feed network position[9]. The design of dual channels with multi-layer may cause cross-polarization radiation [10]. Additionally, asymmetry of the current distribution flows on the patch will lead to higher coupling and generates cross polarization pattern [11]. The last reason is related to shifting of the reference axis.

III. Design of Symmetric and Asymmetric Shapes About Y-axis of Metamaterial Unit Cells

The symmetric shape of CRLH-TL unit cell is designed about the y-axis. It works as feed line and phase shifter simultaneously. The top view of the symmetric 1.5 CRLH-TL metamaterial unit cell is plotted in Fig. 2(a). The structure of the unit cell is consistent with two series IDC with eight digits and two shunt stub inductors at both sides about the y-axis, each stub inductor is shorted through a via to the ground. The field distribution is shown in Fig. 2(b); that illustrates the electric fields are confined in the IDC, which implies that there are high concentrations of field strength in the IDC region. Fig. 2(c) reflects the practical symmetric T-network metamaterial unit cell. The dispersion diagram for the design of 1.5 CRLH-TL unit cell is shown in Fig. 2(d). It is observed that the dispersion diagram is balanced, which implies that $w_{se}=w_{sh}=w_0=10$ GHz. The dispersion diagram displays three distinct frequency regions: left handed, zero order and right handed regions.

Fig. 2(e) shows that $|S_{11}|$ and $|S_{21}|$ of the proposed unit cell; it is found that S_{11} of -35.4 dB and S_{21} of -1 dB at the transition frequency of 10 GHz. Fig. 2(f) shows the phase shift of S_{21} for unit cell only and the total structure (i.e., unit cell plus two transmission lines). It is observed that the phase shift of unit cell of 0° at the transition frequency whereas the phase shift of the total structure is -60° due to extra two transmission lines at the both ends. The Bloch impedance for the unit cell is equal to 50.3 Ω at the transition frequency of 10 GHz as depicted in Fig. 2(g).

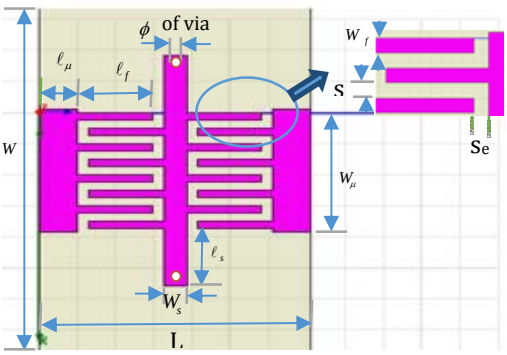

Figure 2. (a), continued on next page

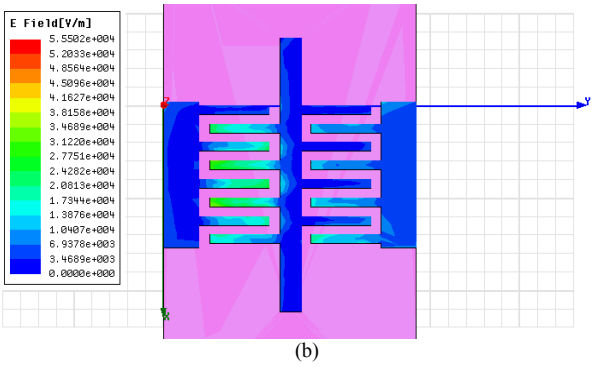

(b)

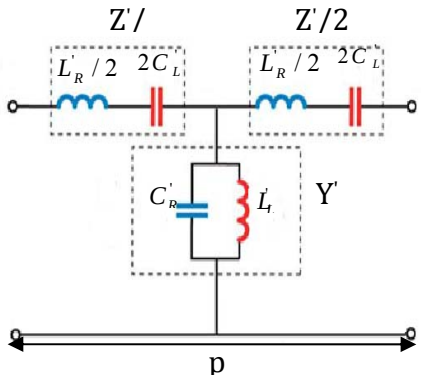

(c)

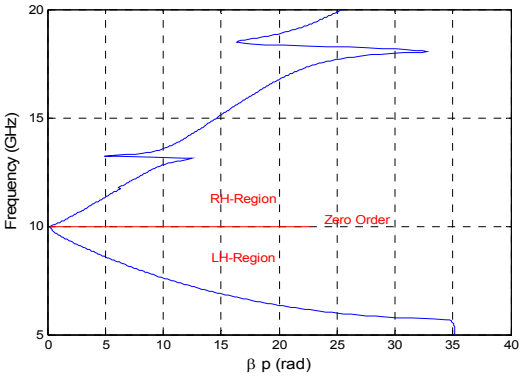

(d)

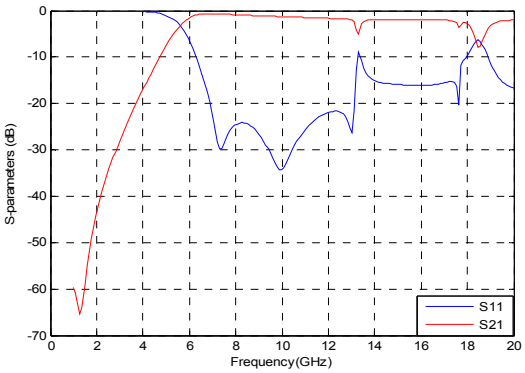

(e)

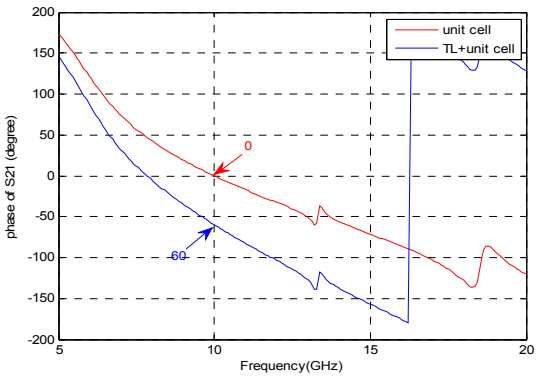

(f)

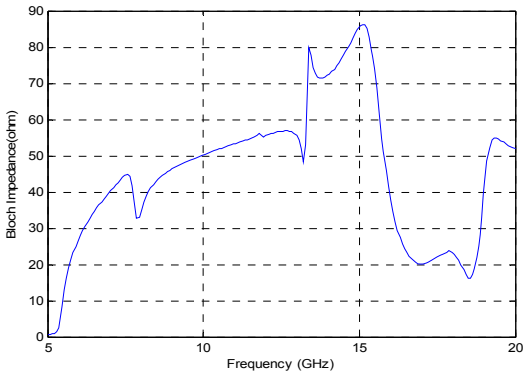

(g)

Figure 2. Design of symmetric 1.5 unit cell CRLH-TL a) 2D Geometry of unit cell CRLH-TL b) field distribution on unit cell c) equivalent circuit for unit cell d) dispersion diagram e) Transmission and reflection coefficients for unit cell f) Phase of S_{21} for unit cell at phase is equal to 0° g) Bloch impedance.

Alternatively, the second part is related to the design of asymmetric metamaterial unit cell. Fig. 3(a) illustrates the proposed top view of asymmetric 1.5 CRLH-TL metamaterial unit cell structure which consists of the two series IDC; each one has three unequal fingers in width and one shorted stub through via to the ground. The E-field distribution on unit cell and the equivalent symmetric T-network are shown in Fig. 3(b and c), respectively. The dispersion diagram for the design of 1.5 CRLH-TL metamaterial unit cell is shown in Fig. 3(d). It is observed that the dispersion diagram is balanced, which means that $w_{se}=w_{sh}=w_0=10$GHz. Fig. 3(e) shows the reflection (S_{11}) and transmission (S_{21}) coefficients of 1.5 CRLH-TL unit cell; it is found that S_{11} of -20.3 dB and S_{21} of -2.22 dB at the resonance frequency of 10 GHz. Fig. 3(f) shows the phase shifts of S_{21} for unit cell only and the total structure. It can be seen that the phase shift of metamaterial unit cell only of 0° at the center frequency whereas the phase shift of entire structure is -55.6°. It can be seen from Fig. 5.13(g) that the Bloch impedance is 48 Ω at 10 GHz.

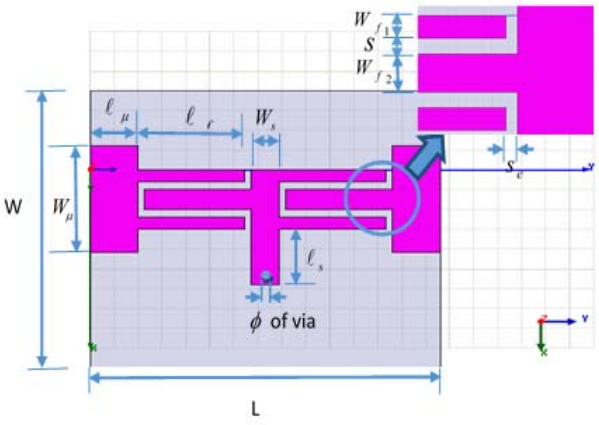

(a)

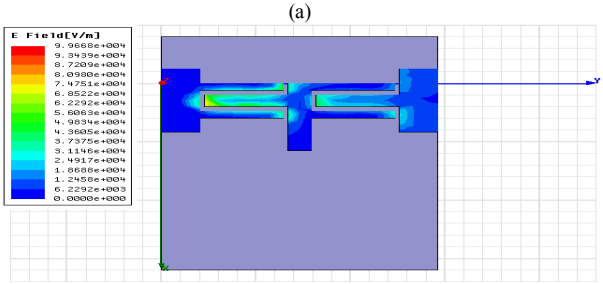

(b)

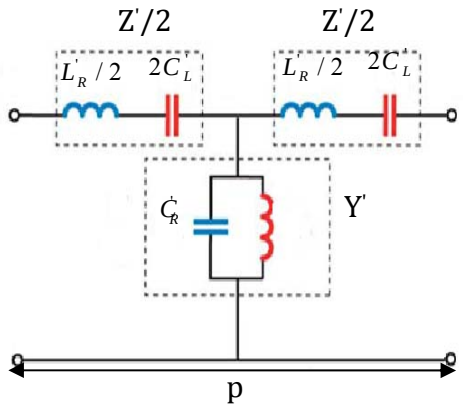

(c)

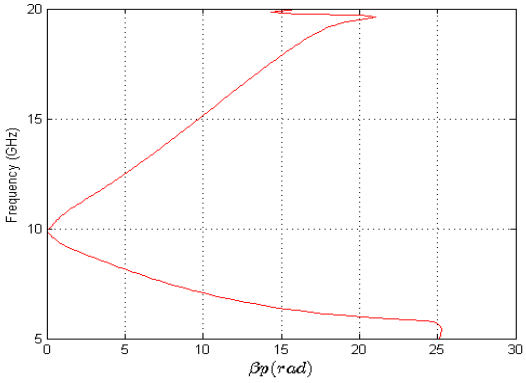

(d)

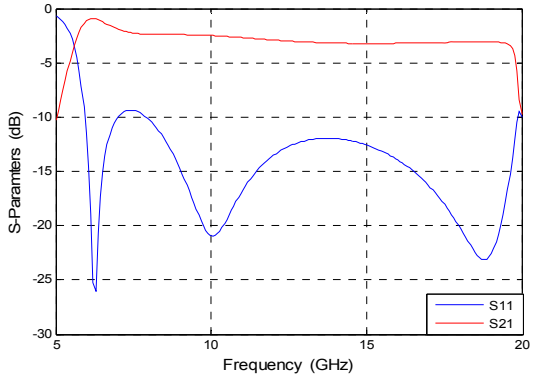

(e)

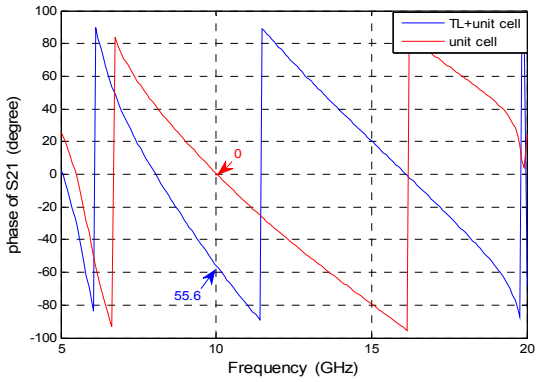

(f)

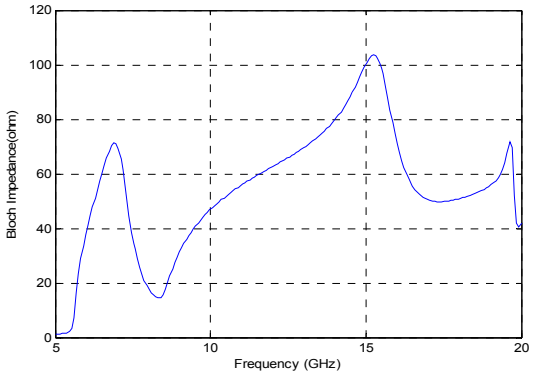

(g)

Figure 3. Design of symmetric 1.5 unit cell CRLH-TL a) 2D Geometry of unit cell CRLH-TL b) field distribution on unit cell c) equivalent circuit for unit cell d) dispersion diagram e) Transmission and reflection coefficients for unit cell f) Phase of S_{21} for unit cell at phase is equal to 0° g) Bloch impedance.

IV. DESIGN OF METAMATERIAL UNIT CELL AS PHASE SHIFTER

From the phase characteristic of symmetric 1.5 unit cell of 40° phase shift with lumped elements are L_R of 3.373 nH, C_L of 0.078 pF, L_L of 0.275 nH, and C_R of 0.895 pF. CRLH-TL is applied to the structure, and design equations are

presented for the calculation of any arbitrary phase shift. The period length of symmetric 1.5 unit cell is 5.1 mm, and it can achieve different values of phase shift without changing the period length. In contrast, there is a linear relation between the length and phase shift, in the case of the transmission line. In addition, CRLH-TL metamaterial can generate positive, zero, and negative phase shift, while in the case of the transmission line can only generate negative phase shifts. Fig. 4 shows the relation between the phase of S_{21} and frequency with different values of phases for the symmetric unit cell at the frequency of 10 GHz. Table I lists the dimensions of CRLH-TL unit cell at phase shifts of 0º and 40º, respectively. The permittivity and permeability can be calculated from utilizing of extracted LC-parameters and depending on the following equations [12][13].

$$\varepsilon = \varepsilon(\omega) = C_R' - \frac{1}{\omega^2 L_L'} = C_R'\left(1 - \frac{\omega_{sh}^2}{\omega^2}\right) \quad (2)$$

$$\mu = \mu(\omega) = L_R' - \frac{1}{\omega^2 C_L'} = L_R'\left(1 - \frac{\omega_{se}^2}{\omega^2}\right) \quad (3)$$

Figure 5(a and b) shows the permittivity and permeability various frequency; it is noticed that both values of permittivity and permeability are negative below the transition frequency and positive above the transition frequency of 10 GHz.

In the case of an asymmetric design, and from the phase characteristic of an asymmetric 1.5 unit cell of 40º phase shift with lumped elements are L_R of 5 nH, C_L of 0.052 pF, L_L of 0.41 nH, and C_R of 0.61 pF. The period length of an asymmetric 1.5 unit cell is 5.3 mm. Fig. (6) shows the relation between the phase of S_{21} and frequency with different values of phases for an asymmetric unit cell at a frequency of 10 GHz. Fig. 7(a and b) shows the permittivity and permeability various frequency; it is noticed that both values of permittivity and permeability are negative values below the transition frequency and positive values above the center frequency of 10 GHz.

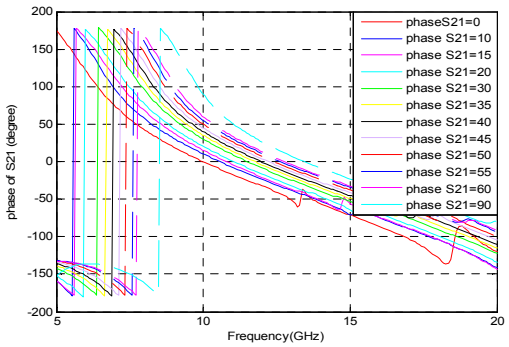

Figure 4. Phase response with various phase shifts for the symmetric unit cell at a center frequency of 10 GHz.

TABLE I. DIMENSIONS OF SYMMETRIC UNIT CELL CRLH-TL AT PHASE SHIFTS OF 0º AND 40º (ALL DIMENSIONS IN MM).

parameters	Phase shift at 0º	Phase shift at 40º
ℓ_μ	1	1
W_μ	3.94	3.94
ℓ_f	1.96	1.513
W_f	0.24	0.2
ℓ_s	1.84	1.53
W_s	0.6	0.6
s	0.26	0.3
s_e	0.3	0.727
p	5.1	5.1
Diameter of via	0.24	0.24

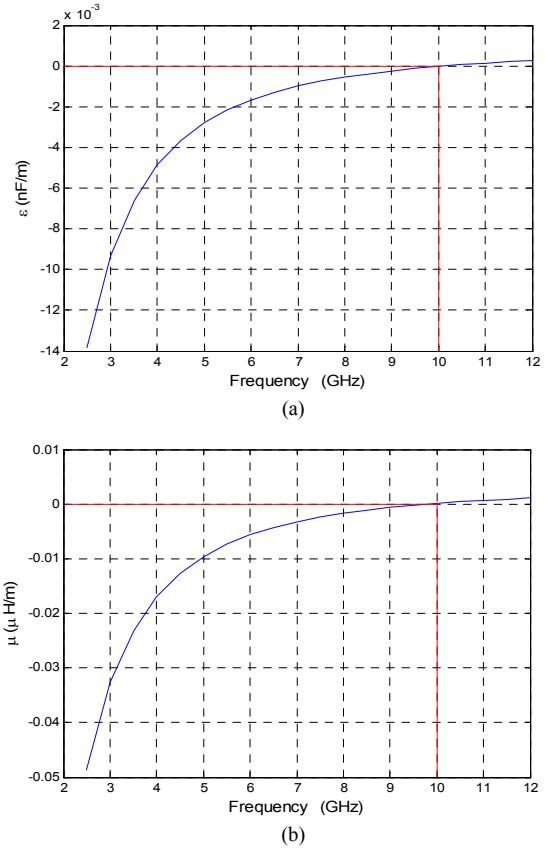

Figure 5. Real values of permittivity and permeability a) Permittivity b) permeability for various frequency for the symmetric unit cell.

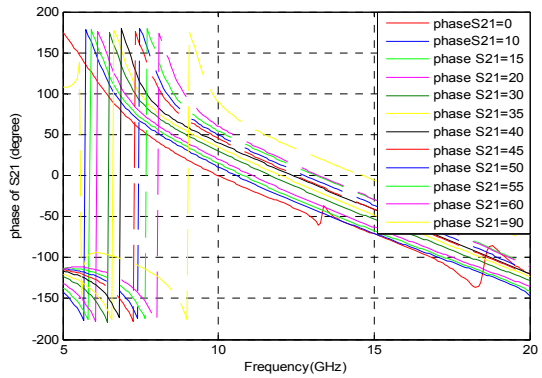

Figure 6. Phase response with various phase shifts for the asymmetric unit cell at a center frequency of 10 GHz.

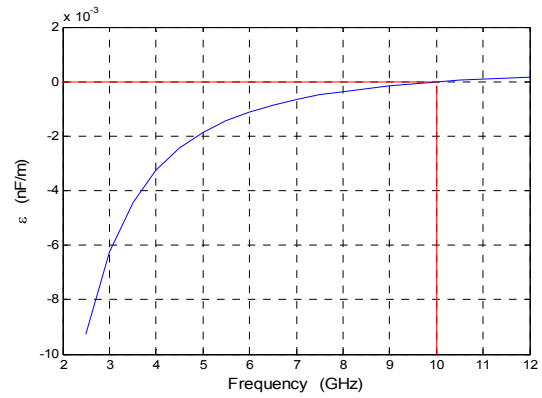

(a)

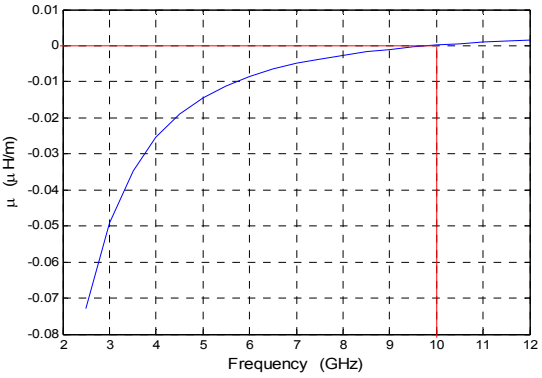

(b)

Figure 7. a) Permittivity b) permeability for various frequency, at a phase shift of 40° for the asymmetric unit cell.

V. THE DESIGN OF DUAL LINEAR POLARIZED RECTANGULAR MICROSTRIP ANTENNA

The proposed antenna geometries at 10GHz for symmetrical and an asymmetrical configurations are presented in Fig. 8(a) and (b), respectively. Fig. 8(c) shows the explode 3D geometry of antenna system. The antenna has two substrate layers and three metal layers. The rectangular microstrip patch antenna is printed with metamaterial feed line on the first substrate layer. The feeding networks consist of two orthogonal hybrid feeds. The first port is MTM line which is associated with horizontal polarization (excites the linearly polarized radiation along the yz- plane). It is considered coplanar feed for rectangular patch antenna that is printed with MTM feed line on the first substrate layer to function as a phase shifter.

The second port is aperture coupling microstrip line which is associated with vertical polarization (excites linearly polarized radiation along the xz-plane) and printed on the bottom of the second substrate layer. The advantage of using aperture coupling that does not require the soldering process as in coaxial cable feeding. The length and the width of the microstrip feed line have been tuned so that the input impedance is ~50Ω.

The antenna structure consists of two substrate layers. The first substrate supports the rectangular patch and MTM line. It is used Roger RT/duroid 5880 substrates of height 1.575 mm, relative permittivity 2.2, and excellent dissipation factor tan δ=0.0009 for good antenna efficiency performances. The second substrate or aperture feed substrate used Rogers RO4350 substrate of thickness 0.508 mm and relative permittivity 3.48. The thickness of patch and two feeds is 35 µm. The gap "g" is inserted between CRLH-TL unit cell and radiating patch. The purpose from the gap is for coupling and improving the return loss. The ground plane is inserted between two substrate layers which contain the slot, the purpose of the position is to prevent the radiation from microstrip line interfering with microstrip radiation pattern. Table II lists the details dimensions of antenna system for symmetric and asymmetric configurations.

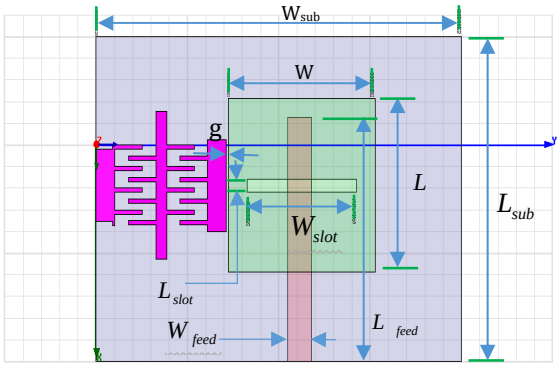

(a)

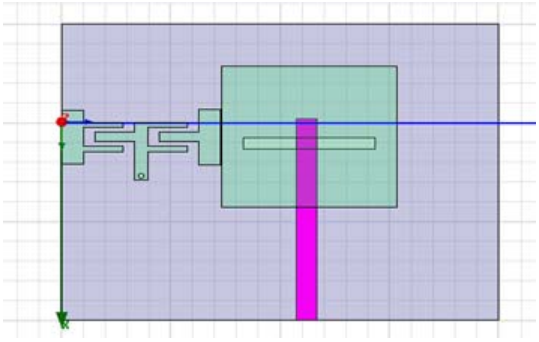

(b)

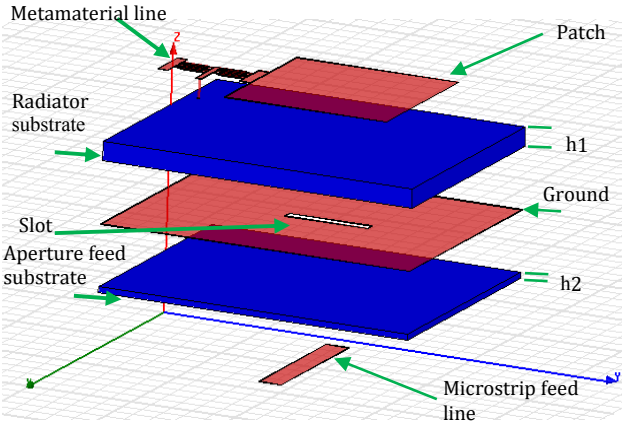

(c)

Figure 8. The geometry of antenna design a) 2D geometry of symmetric design b) 2D geometry of an asymmetric design c) 3D geometry.

TABLE II. PARAMETERS VALUES OF A DUAL LINEAR POLARIZATION ANTENNA SYSTEM FOR SYMMETRIC AND ASYMMETRIC DESIGNS (ALL UNITS IN MM).

parameters	symmetric	asymmetric
W	7.97	8.03
L	7.1	8.03
W_{sub}	20	20
L_{sub}	15	15
W_{feed}	0.95	1.3
L_{feed}	10.2	11.25
W_{slot}	6	6
L_{slot}	0.6	0.6
Gap (g)	0.07	0.111

VI. RESULTS AND DISCUSSION

The characteristics of a dual linear polarization antenna using hybrid feed have been studied. A conventional dual linear polarization antenna is shown in Fig. 9, which operates at the frequency of 10 GHz with dimensions of ℓ=5mm, ℓ_q is quarter wave transformer= 5.84mm, ℓ_f=15 mm, W=8.32 mm and L=8.24 mm. Fig. 10 displays the simulation transmission coefficients (S_{11} and S_{22}) for two ports, and the mutual coupling coefficients (S_{21}). The simulation reveals that S_{11}=-36 and -21.5 dB, S_{22}=-28 and -40 dB, and the isolation between two input ports is found to be -30 and -27.1 dB for two antennas, i.e., the proposed one and the conventional antenna, respectively. The simulated antenna offers bandwidth of 8% and 8.2% for horizontal and vertical ports, respectively. Fig. 11(a and b) shows the linear form of co-cross polarization patterns in E and H-planes of two antennas for the horizontal port. Good XPD is observed and is equal to 34 dB at broadside direction. On the other hand, the XPD of the conventional antenna about 27 dB.

In the case of an asymmetric arrangement, the theoretical results of the transmission coefficients (S_{11}, S_{22}), and the mutual coupling coefficients of the antenna (S_{21}) at port V and H are shown in Fig. 12. S_{11} is equal to -11.5 dB, S_{22} is equal to -28 dB, and the isolation between two input ports is seen to be -29 dB at the centre frequency. Fig. 13(a and b) shows the co and cross polarization patterns in E and H-planes for the horizontal port. Good XPD is observed and is equal to 32.7 dB at the broadside direction at a phase shift of 40°. A 3D polar pattern for dual linear polarization antenna is shown in Fig. 13(e).

The gain has been calculated versus frequency for three antennas (conventional, proposed symmetric and asymmetric antennas), as shown in Fig. 14. It can be recognized that the gain of the proposed antennas declines rapidly after the frequency of 10.7 GHz, so the gain is not important out of this range. Finally, Table III summarizes the performance characteristics of the conventional and proposed dual linear polarization antennas for comparison. It is noticed that the newly proposed antenna is better than the conventional antenna in term of isolation, XPD and S-parameters. The proposed antenna is seen to have an excellent radiation efficiency of 99.6%.

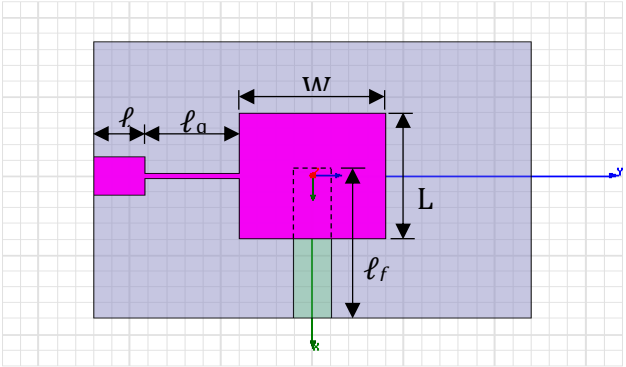

Figure 9. 2D Conventional dual polarization antenna with hybrid feeds (coplanar and coupling aperture feeds).

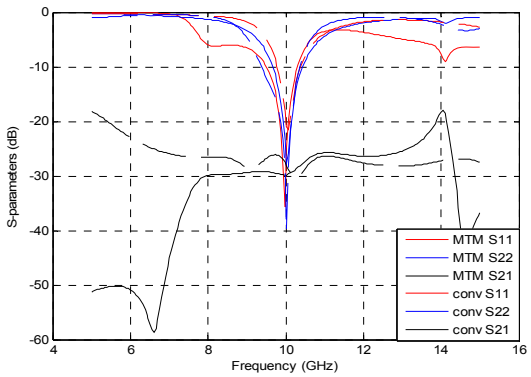

Figure 10. The transmission coefficient for two ports and mutual coupling coefficients of the antenna (S_{11}, S_{22}, and S_{21}) for symmetric design.

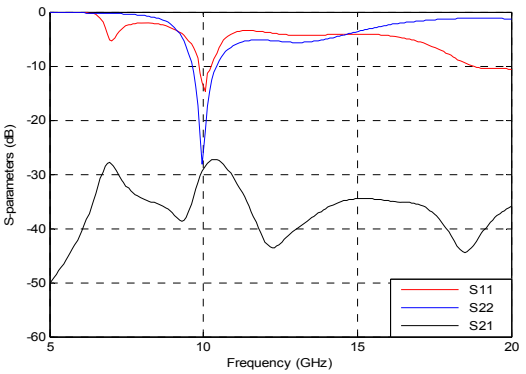

Figure 12. The transmission coefficient for two ports and mutual coupling coefficients of the antenna (S_{11}, S_{22}, and S_{21}) for an asymmetric design.

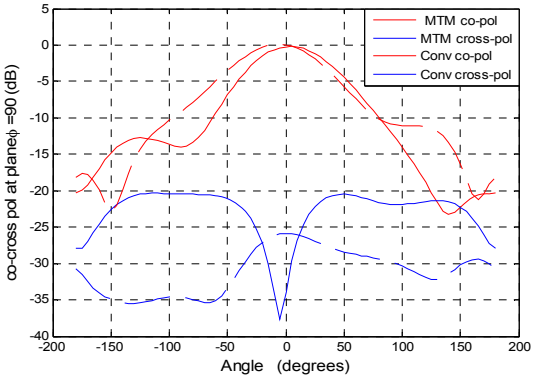

(a)

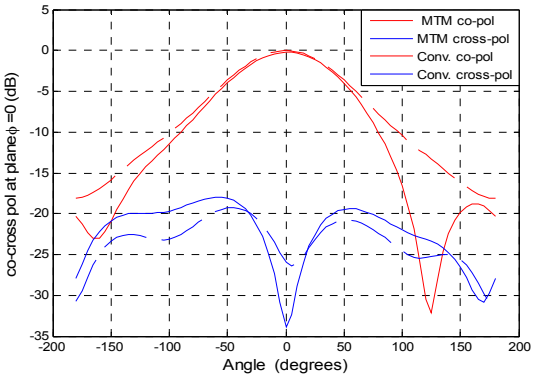

(b)

Figure 11. The Linear plot for Co-Xol radiation pattern of the proposed symmetrical dual linear polarization and conventional antennas for H-port in a) E-plane and b) H-plane.

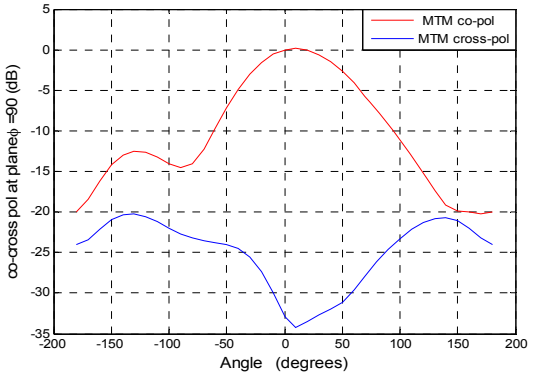

(a)

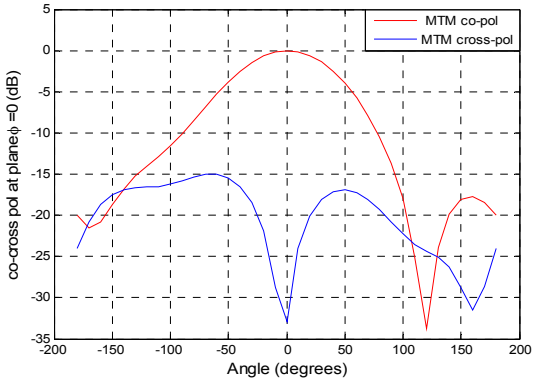

(b)

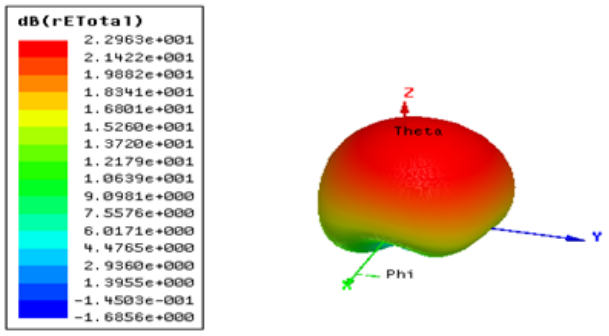

(e)

Figure 13. The Linear plot for co-cross radiation pattern of the proposed asymmetrical dual linear polarization and conventional antennas for H-port in a) E-plane and b) H-plane.

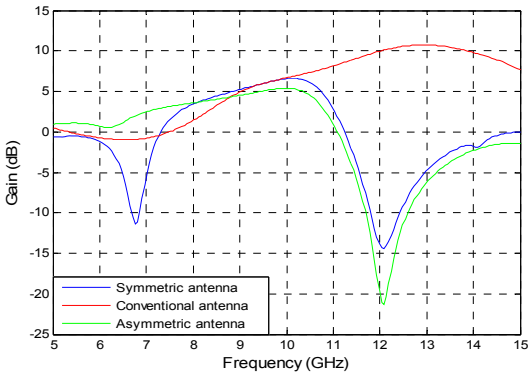

Figure 14. Gain versus frequency for three antennas (conventional and proposed symmetric and asymmetric antennas).

TABLE III. COMPARISON BETWEEN THE CONVENTIONAL AND PROPOSED DUAL LINEAR POLARIZATION ANTENNAS.

Parameters	Conventional Antenna	Proposed Symmetric Antenna	Proposed Asymmetric Antenna
S_{11} (dB)	-21.5	-36	-14.5
S_{22} (dB)	-40	-28	-28
S_{21} (dB)	-27.4	-30	-29
XPD (dB)	27.5	34	32.7
G (dB)	6.68	6.65	5.67
BW_1 (GHz)	0.603	0.8	0.41
BW_2 (GHz)	0.994	0.82	0.798
e %	99.3	99.6	99.3

VII. THE EFFECTS OF PHASE SHIFT ON ISOLATION AND CROSS POLARIZATION

This section deals with the investigation the effects of phase shifts on mutual coupling, cross polarization patterns, and the other characteristics such as gain and bandwidth for symmetric and asymmetric configurations. Figure 15(a and b) shows the effect of the phase shift on the cross-polarization radiation patterns in principle planes at different phase shifts (0, 90º). Relatively smaller cross-polarization radiation patterns and symmetric about the broadside are observed in H-plane. Figure 16(a) shows the relation between the XPD and phase shift. It is observed that the XPD becomes the best value of 34 dB at a certain phase shift of 40º and they tend to become the worst values at advance in phase shift beyond the phase shift of 40º. Figure 16(b) illustrates the relation between isolation and phase shift; it is noticed that the coupling is oscillated between -29 and -33 dB within these values of phase shifts. The simulated 10 dB return loss bandwidth for two ports with various values of the phase shift is depicted in Fig. 17(a). It is noticed that the bandwidth for horizontal-port reduce with increasing of phase shift while the bandwidth of vertical-port remains approximately constant. The relation between the gain and phase variation is illustrated in Fig. 17(b). It can also be seen that the gain is reduced by increasing the phase shift, about 0.5 dB along 90º phase shift.

In the case of asymmetric design, Fig. 18(a and b) show the effect of the phase shift on the cross-polarization radiation in principle planes at different phase shift. It is recognized that at a phase shift of 40º has the high XPD of 32.7 dB at the broadside and high isolation of -29 dB at the center frequency. Fig. 19(a) shows the relation between the XPD and phase shift. It is observed that the XPD becomes the best value at a certain phase shift of 40º and they tend to become the worst values at advance the phase shift beyond the phase shift of 40º. The isolation of an asymmetric design is about -28 to -31 along the phase shift of 50º and become worse value as increasing of phase shift after this phase shift, as illustrated in Fig. 19(b). Fig. 20(a) shows the simulated 10 dB return loss bandwidth for two ports with various values of the phase shift; it is noticed that the bandwidth for horizontal -port reduce with increasing of phase shift while the bandwidth of vertical-port remains approximately constant. Fig. 20(b) shows the relation between the gain and phase variation.

It can be seen from these results that the cross polarization patterns at E-plane (in the case of symmetric arrangement) are offset from the broadside as shown in Fig. 15(a). Moreover, they have the minimum values at an angle of θ=-10º. On the other hand, it can be observed from Fig. 18(a), in the case of asymmetric design, the cross polarization patterns at E-plane have large offset angles from the broadside and they have the minimum values at angles of θ≈60º or greater. From Fig. 15(b), it can be recognized that the cross polarization patterns in H-plane are symmetric about the broadside (in the case of symmetrical design). Whereas, Fig. 18(b) shows the cross polarization patterns for asymmetric configuration, which are offset from the broadside and they have the minimum values at an angle of θ=-10º.

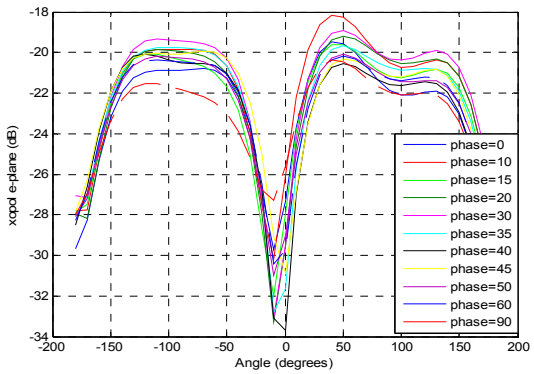

(a)

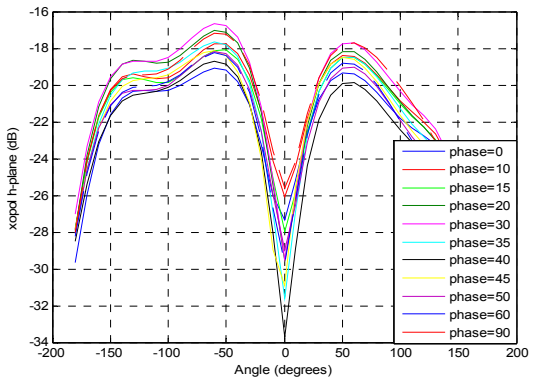

(b)

Figure 15. The Linear plot for cross-polarization in E and H –planes for different values of phase for H-port (0º- 90º).

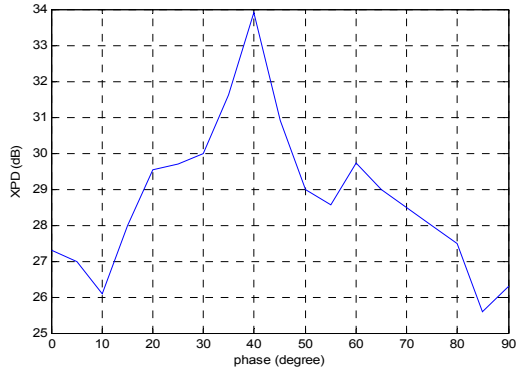

(a)

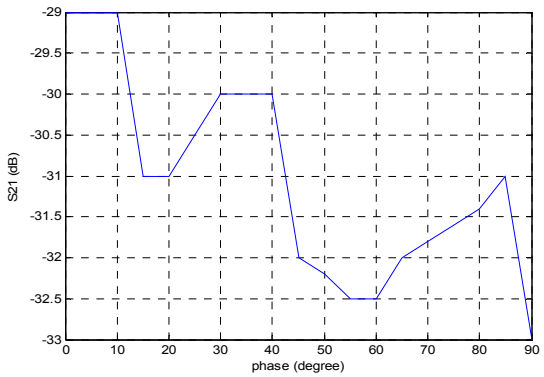

(b)

Figure 16. The relation between phase shift and a) XPD b) isolation for symmetric case.

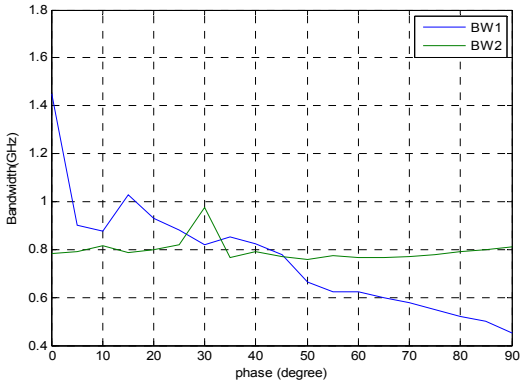

(a)

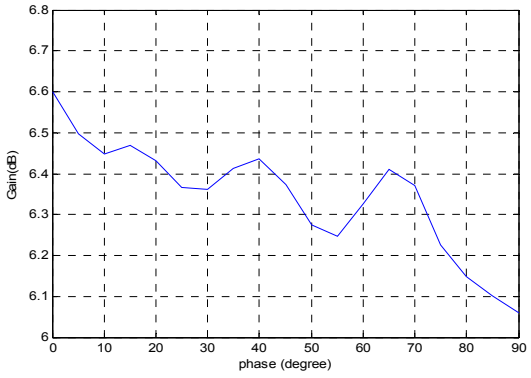

(b)

Figure 17. The relation between phase shift and a) Bandwidth b) Gain for symmetric case.

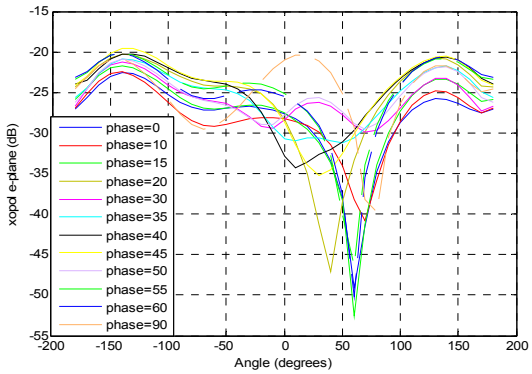

(a)

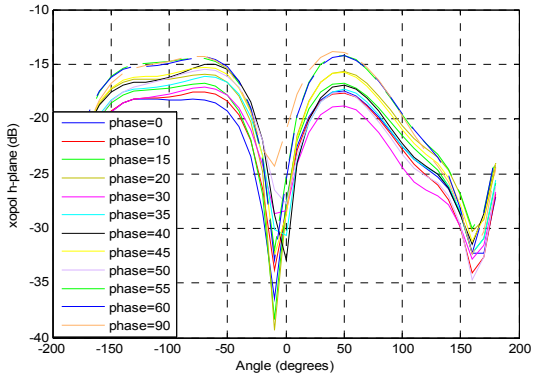

(b)

Figure 18. The Linear plot for X-pol in E and H –planes for different values of phase for H-port (from 0º to 90º).

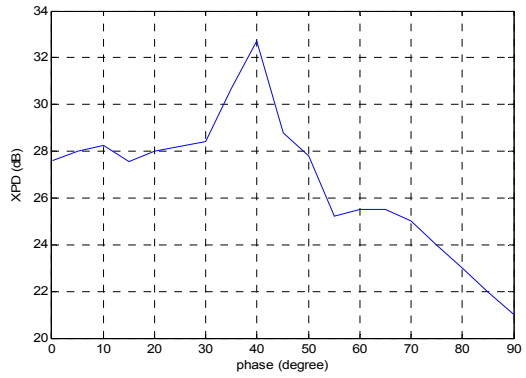

(a)

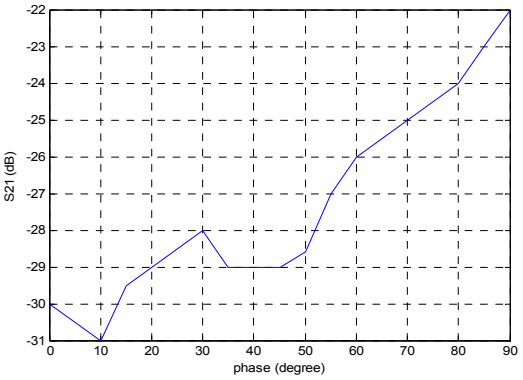

(b)

Figure 19. The relation between phase shift and a) XPD b) Isolation for asymmetric case.

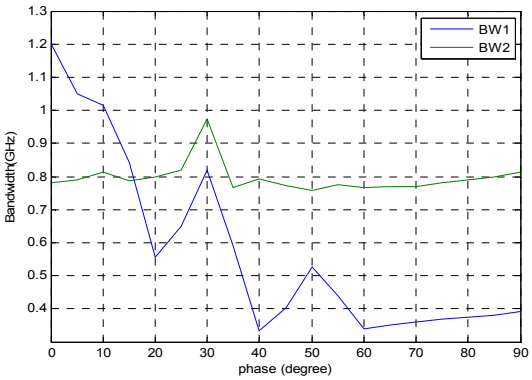

(a)

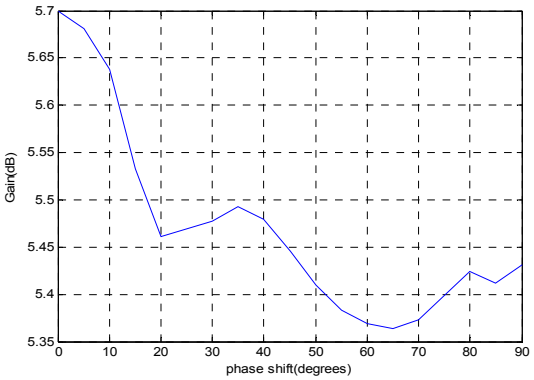

(b)

Figure 20. The relation between phase shift and a) Bandwidth b) Gain for asymmetric case.

VIII. CONCLUSIONS

Dual linear polarization antennas have been designed using symmetrical and asymmetrical metamaterial unit cells. This work has been studied the effects of positive phase shift which is generated by CRLH-TL metamaterial on the XPD and isolation. The simulation results achieved high XPD and high isolation of dual linear polarization microstrip antenna. It is found that at a phase shift of 40^{o} the XPD of 34 dB and isolation of -30 dB. The simulation reveals an improvement in the XPD by 7 dB as compared with conventional design at broadside. Furthermore, study the effect of symmetrical and asymmetrical unit cells on the cross polarization patterns in principle planes is achieved. It is found that the cross polarization pattern is symmetric about the broadside at H-plane in the case of using symmetrical unit cell.

REFERENCES

[1] K. Luo, W. Ding, Y. Hu, and W. Cao, "Design of Dual-Feed Dual-Polarized Microstrip Antenna with High Isolation and Low Cross-Polarization,", Progress In Electromagnetics Research Letters, vol. 36, no., pp. 31–40, November 2013.

[2] K. Wong, and T. Chiou, "Broad-Band Dual-Polarized Patch Antennas Fed by Capacitively Coupled Feed and Slot-Coupled Feed," IEEE Transactions on Antennas and Propagation, vol. 50, No. 3, March 2002.

[3] T. Chiou and K. Wong, "Broad-Band Dual-Polarized Single Microstrip PatchAntenna With High Isolation and Low Cross-Polarization," IEEE Transactions on Antennas and Propagation, vol. 50, No. 3, March 2002.

[4] S. Gao, L. W. Li, M. S. Leong, and T. S. Yeo," A Broad-Band Dual-Polarized Microstrip Patch Antenna With Aperture Coupling," IEEE Transactions on Antennas and Propagation, vol. 51, No. 4, April 2003.

[5] B. Lindmark, "A novel dual polarized aperture coupled patch element with a single layer feed network and high isolation," IEEE Antennas Propag. Soc. Int. Symp. 1997. Dig., vol. 4, pp. 2190–2193, 1997.

[6] " Definitions of Terms Relating to Propagation in Non-Ionized Media," Radio Communication Study Group 3 made editorial amendments to this Recommendation in 2000 in accordance with Resolution ITU-R 44.

[7] L.J. Ippolito and R.D. Kaul,"Propagation Effects Handbook for Satellite System Design," Nasa Reference Publication, Second edition, 1981.

[8] X.-L. Liang, S.-S. Zhong, and W. Wang, "Design of a dual-polarized microstrip patch antenna with excellent polarization purity," Microw. Opt. Technol. Lett., vol. 44, no. 4, pp. 329–331, Feb. 2005.

[9] V. I. C. Onclusion, "Dual-Feed Dual-Polarized Patch Antenna With Low Cross Polarization and High Isolation," IEEE Trans. Antennas Propag., vol. 57, no. 10, pp. 3405–3409, 2009.

[10] W. L. Stutzman and G. A. Thiele," Antenna Theory and Design," Second edition, John Wiley and Sons,1998.

[11] M. Barba, "A High-Isolation, Wideband and Dual-Linear Polarization Patch Antenna," IEEE Transactions on Antennas and Propagation, vol. 56, no. 5, pp. 1472–1476, 2008.

[12] C. Caloz, and T. Itoh, "Electromagnetic Metamaterials: Transmission Line Theory and Microwave Applications," John Wiley & Sons, 2006.

[13] C. Calm, T. Itoh, and A. Rennings, "CRLH Metamaterial Leaky-Wave and Resonant Antennas," IEEE Antennas and Propagation Magazine, Vol. 50, No. 5, pp. 25–39, October 2008.